JETIR.ORG ISSN: 2349-5162 | ESTD Year : 2014 | Monthly Issue
JOURNAL OF EMERGING TECHNOLOGIES AND INNOVATIVE RESEARCH (JETIR)
An International Scholarly Open Access, Peer-reviewed, Refereed Journal

Fluorescence "Off-On" recognition system of Tween- 80 stabilized 9-Anthracene Carboxylic Acid Nanoparticles for CN^-: Application to Environmental Analysis

D. K. Dalavi
Associate Professor
Department of Chemistry,
Bhogawati Mahavidyalaya, Kurukali.
Affiliated to Shivaji University, Kolhapur.

ABSTRACT:

The aqueous suspension of tween-80 stabilized anthracene nanoparticles was prepared by reprecipitation method and designed fluorescent 'Off-On' T80-9-ACANPs based nanosensor for recognizing hydroxocobalamin and cyanide ion (CN^-) in aqueous media. The blue-shifted absorption band of T80-9-ACANPs due to H-aggregated nanostructures shows AIEE at λ_{max} = 412 nm due to hindered molecular rotations favoring radiative decay of nanoaggregates. The effect of interfering substances on the enhancement capacity of CN^- examined in the presence of other ions indicated that CN^- response is of high order while other ions responded negligibly. The linear fitting, R^2 = 0.9994 of the 'turn-on' fluorescence which is indicative of a very strong interaction of the fluorophore in the 'Off-On' fluorescence process. The low limit of detection for enhancement was calculated to be 6.87 nM. The possible mechanism of fluorescence enhancement of nanoparticles upon interaction with CN^- was discussed on the basis of ground state complex formation. Further, the proposed fluorescence enhancement method was successfully applied for the detection of CN^- in urine and environmental samples by standard addition method.

1. INTRODUCTION

Fluorescent Organic Nanoparticles (FONPs) have created considerable interest since last decade owing to selective binding ability towards analyte molecules. FONPs have inspired growing research efforts due to great diversity of organic molecules available, the flexibility in material synthesis, good water solubility and optical properties.[1-8] Inorganic materials and metal nanoparticles are reported successively in recent years but least attempts have been made to design and characterize the FONPs. The methods of preparation of inorganic and metal nanoparticles are lengthy, complicated and expensive. In contrast preparation of fluorescent organic nanoparticles is simple, quick and cost effective method. It is known that water insoluble organic molecules having non-bonded electron pair with heteroatom and electropositive hydrogen atom in functional moiety on phenyl ring can undergo hydrogen bonding in aqueous medium to form dimer. The careful nucleation in aqueous medium of such compounds from their homogeneous solution in volatile solvent can give nanoparticles due to aggregation. Hence, with a hope to obtain nanoparticles exhibiting aggregation-induced enhanced emission (AIEE)[6-10] the fluorescent 9-Anthracene carboxylic acid (9-ACA) was chosen for preparation of nanoaggregates by reprecipitation method and as per expectation aqueous suspension of nanoparticles exhibiting blue shifted enhanced emission was achieved.

Anions play vital role in several ecological, aquatic and catalysis methods.[11] Among them, cyanide as one of the valuable anions in diverse fields such as the removal of silver or gold process,[12] electroplating, acrylic fiber and resin manufacturing, metallurgy and herbicide production.[13] CN^- is one of the most hazardous anions owning to its lethal actions in spite of their valuable properties.[14, 15] Key sources of cyanide containing substances are ground water, soil, contaminated air, vehicle exhaust and cigarette flaming gas. These are extremely harmful to human beings and most animals by causing lethal damage to their nervous systems.[16, 17] The human toxicity of which being related to its ability

to bind cytochrome c oxidase that causes the inhabitation of oxygen transport to mitochondria and resulting in hypoxia.[18] According to the WHO, water having cyanide concentrations lower than 1.9 μM are acceptable for drinking. Some studies have shown that the poisonous cyanide concentration in the blood of fire victims is 20 μM.[17] Thus, owing to its high toxicity and extensive use in industrial processes, designing of selective and sensitive methods for the determination of low levels of CN^- is of significantly importance. Various analytical methods have been utilized for the determination of CN^- including colorimetric,[19, 20] chemodosimeter,[21] chromatographic,[22] piezoelectric quartz crystals,[23] ratiometric fluorescence,[24] fluorimetric[25, 26] and spectrophotometric[27] methods. In this context, various types of fluorimetric and colorimetric CN^- selective receptors have been reported based on the mechanism of coordination, hydrogen-bonding interactions, nucleophilic addition reactions, or metal-cyanide affinity. Among them, the proposed method based on 'Off-On' fluorescence nano sensor offer the opportunity for a highly sensitive, simple, cheap and easy detection of CN^-.

2. EXPERIMENTAL:

2.1 Equipments

The absorption spectrum was acquired at room temperature on a UV-3600 Shimadzu UV-VIS-NIR spectrophotometer using a 1.0 cm quartz cell. The fluorescence measurement of the solutions was carried out using a PC based spectrofluorophotometer (JASCO Model FP-8300, Japan). The excitation wavelength of 352 nm and emission wavelength of 412 nm of aqueous suspension was obtained from their excitation and the emission spectrum respectively. Both the excitation and emission slits were fixed at 5 nm. The particle size distribution and zeta potential of (Tween 80 stabilized 9-ACANPs) T80-9-ACANPs in aqueous suspension was measured by Dynamic Light Scattering (DLS) with a Zeta Sizer Nano ZS (Malvern) Instruments limited U. K. The fluorescence lifetimes in the time scan 500 ps to 1μs are measured by Time Correlated Single Photon Counting (TCSPC) method of Horiba Sci. NL (Japan) at emission and excitation of wavelengths 412 nm and 360 nm respectively. The pH of solutions was measured with a digital pH meter, model LI–120 (ELICO Hyderabad, India.), with a combined glass electrode.

2.2 Preparation T80-9-ACANPs by Reprecipitation Method:

The reprecipitation method, which is based on the difference in solubility of the target molecules in two miscible good and poor solvents. The nanoparticles were prepared by injecting 1 mL of 9-ACA solution in acetone (1 mM) into 50 mL aqueous solution of Tween 80 (0.01 mM) under vigorously stirring at ambient temperature. The mixture solution was continually stirred for half an hour and the content was sonicated for 15 min at 301 K to induce dispersion of nano scale size particles into water. In aqueous medium, 9-ACA molecule nucleates and self-assembled in aggregates to give nanoparticles in aqueous suspension.

3. RESULTS AND DISCUSSION

3.1 PARTICLE SIZE DISTRIBUTION OF 9-ACANPS:

The size distribution histogram of nanoparticles in aqueous suspension was recorded by dynamic light scattering (DLS) technique. Fig. 1 exhibits the particle size distribution of T80-9-ACANPs. The particle size data shows a range of particle size from 32.67 nm to 190.1 nm and a distribution of mean of particles from 9.5 % to 0.9 %. The maximum mean is 27.3 %, however, 53.7 % distribution of mean of particles within a range of particle size from 37.84 to 50.75 nm and the average particle size is about 43 nm.

3.2 PHOTOPHYSICAL PROPERTIES OF T80-9-ACANPS:

3.2.1 UV-visible Absorption Spectroscopy

The photophysical study of T80-9-ACANPs has provided information in support of the formation of nanoparticles and also helped to explore the suitability of nanoparticles for sensing application. The UV-Visible absorption spectra of dilute solution of 9-ACA in acetone (solid line) and in aqueous suspension (dashed line) are presented in Fig. 2.

Generally, organic molecular aggregates are classified on the basis of the observed spectral shift of the absorption maximum relative to the respective absorption maximum of the monomer.[4,6,28] For the majority of possible dimer geometries, two types of absorption bands arise, one is H-type aggregates *i.e.* absorption band shifted hypsochromically (blue shifted), and other J-type or Scheibe-type aggregates *i.e.* absorption band shifted bathochromically (Red shifted).[29,30] The careful observation of the absorption spectrum of dilute solution of 9-ACA in acetone is banded with peak maxima at 384, 364, 346 and 330 nm which are ascribed to 0→0, 0→1, 0→2 and 0→3 transition of which 0→1 being most probable transition, while that of T80-9-ACANPs shows blue shifted spectrum with peak maxima at 376, 356 and 342. The hypsochromic (blue) shift in the absorption band of T80-9-ACANPs as compared to dilute solution of 9-ACA in acetone is an indicative of H-aggregates formed due to strong lateral π-stacking. The π- π interactions allows molecules aligned parallel to each other to form dimer in site of restricted the rotation of phenolic $^-$OH group in aqueous suspension. Hence, blue shift indicates that the molecules undergo H-aggregation in aqueous suspension, presented in scheme 1.

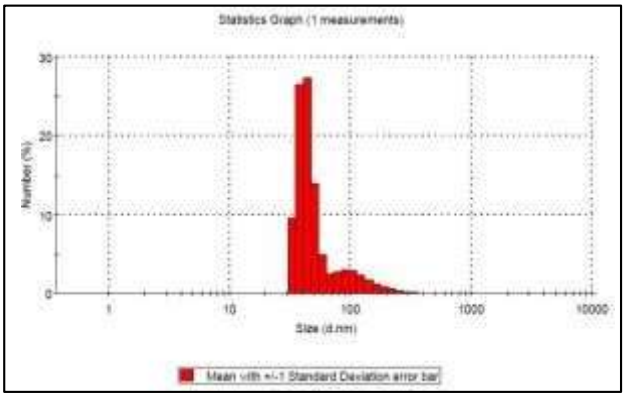

Fig.1: Particle size distribution of T80-9-ACANPs recorded by DLS.

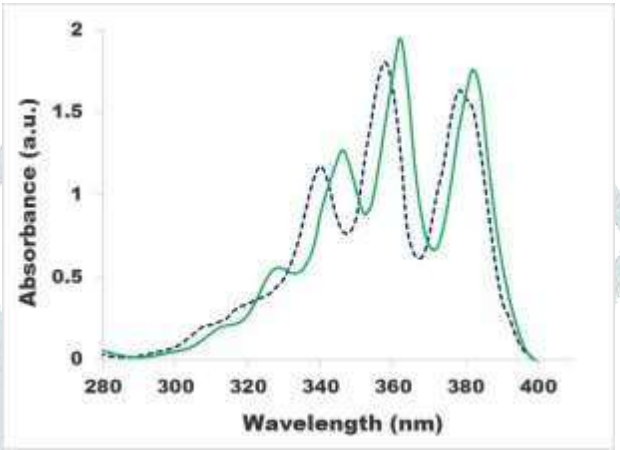

Fig. 2: UV-vis absorption spectra of dilute solution of 9-ACA in acetone (solid line) and T80-9-ACANPs in aqueous suspension (dashed line).

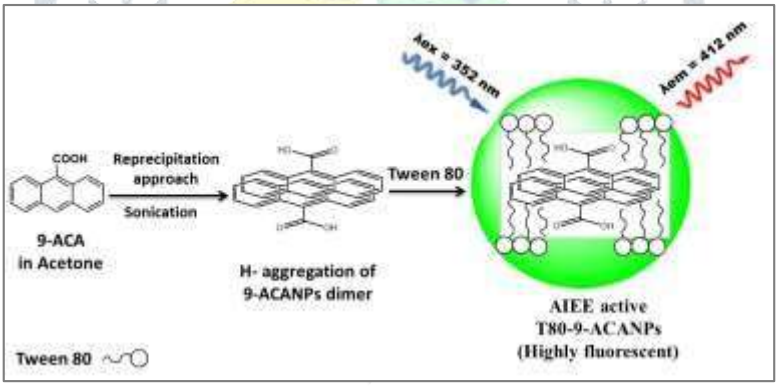

Scheme 1: H-aggregation of T80-9-ACANPs in aqueous suspension.

3.2.2 Fluorescence Spectroscopy:

The aqueous nanoparticle suspension exhibiting narrow particle size distribution in DLS histogram was undertaken for photo-luminescence studies. Fig. 3 presents the emission spectrum of dilute solution of 9-ACA in acetone and in water monitored at the excitation wavelength, λ_{ex}= 360 nm and that of T80-9-ACANPs in aqueous suspension monitored at the excitation wavelength, λ_{ex}= 352 nm.

Careful observation of figure revels that the anthracene like structured emission spectrum of 9-ACA in protic solvent *i.e.* in water while broad emission spectrum in aprotic solvent *i.e.* in acetone (λ_{max}= 457 nm) and less intense as compared to aqueous suspension of T80-9-ACANPs (λ_{max}= 412 nm). 9-ACA has less intense emission, hydrophobic nature and less solubility in water, there are limitations in the use of 9-ACA as a sensor for analysis of water soluble analyte species. In contrast, the structured emission spectrum of T80-9-ACANPs reveals strong AIEE band peaks at 394, 412 and 433 nm, whereas, emission maximum at 412 nm (red solid line). Figure reveals the emission spectrum of nanostructure (λ_{max}= 412 nm) is more intense and strongly blue shifted by 45 nm from the broad, structureless emission of isolated molecules in acetone appeared at 457 nm (blue line). These spectral properties clearly indicate that the blue-shifted emission is because of the aggregated molecules of 9-ACA nanostructure.

AIEE behavior of FONPs mostly originating from the restriction of intramolecular rotation in the aggregation state. In dilute solution, the intramolecular ration is active and internal conversion from a higher to a lower electronic state (nonradiative decay) is much faster than emission. Hence the fluorescence intensity of dilute solution of organic molecules is remarkably quenched. However, in the aggregated state, the nonradiative path is blocked by restricting the intramolecular rotation, which in turn opens up a radiative channel and makes the organic fluorophore extremely emissive.[29]

The emission spectrum of 9-ACA in water has less emissive fingerlike structured emission, however, T80-9-ACANPs exhibits unexpected emissive properties with aggregation enhanced emission which is blue shifted from emission spectrum of 9-ACA in acetone. The restriction of intramolecular rotation of carboxylic group in nanoaggregates was found as a comprehensive mechanism for the AIEE effect, hence, non-radiative pathways becomes radiative. The low emission intensity of dilute solution of 9-ACA molecule in acetone is due to dissipation of energy to molecular rotations.[29]

3.2.3 Selective 'Off-fluorescence' of T80-9-ACANPs by Hydroxocobalamin:

The selectivity and specificity of the fluorescence based T80-9-ACANPs sensor was explored by studying the effect of interfering analyte solutions. The possibility of practical application in the recognition of OHCbl in biofluids and pharmaceutical formulations, the interference from biologically relevant cations and coexisting substances often contained in a sample matrix was tested under the optimal conditions.

Fig. 3 reveals that the fluorescence response of T80-9-ACANPs in the presence of standard OHCbl solution (30.0 μM) is highly selective over some other coexisting substances (100 μM) tested. It appears that the addition of coexisting substances such as sucrose, dextrose, lactose, thiourea, urea, tyrosine, and common metal ions like Hg(II), VB12, Cu(II), Ca(II) quenches the fluorescence to very small extent and in the presence of fructose, maltose, Na(I), Ni(II) and Co(II) slightly enhances the fluorescence inspite of 'Off-fluorescence'. In comparison, OHCbl only induce a sizable quenching effect.

The bar graph presented in Fig. 4 reveals that the fluorescence quenching of T80-9-ACANPs in the presence of standard OHCbl solution (5.0 μM) is highly selective over some other coexisting substances (100 μM) tested. It is of novelty that merely OHCbl exhibiting significant quenching and all others show some extent of fluorescence quenching or enhancement of T80-9-ACANNPs.

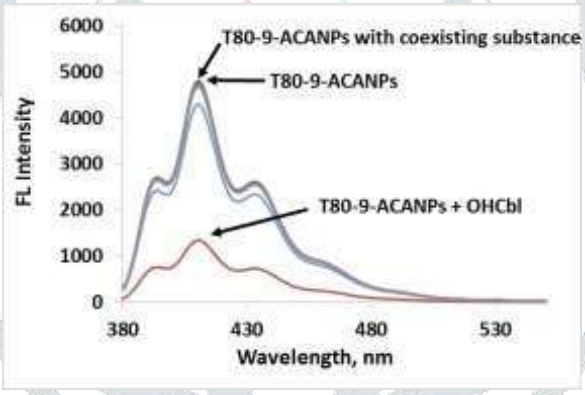

Fig. 3: Selectivity of T80-9-ACANPs towards OHCbl (30.0 μM).

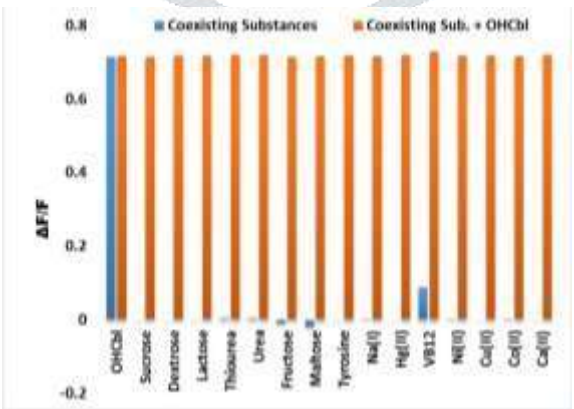

Fig. 4: Effect of coexisting substances on T80-9-ACANPs in presence of OHCbl (5.0 μM).

3.2.4 Fluorescence Quenching of T80-9-ACANPs by OHCbl Solution:

The fluorescence intensity of the probe was significantly quenched regularly without any spectral shift under the gradual addition of OHCbl solution in the concentration range of 0.1–30 μM. The quenching results fit the conventional linear Stern–Volmer relationship (1).

$$\frac{F_0}{F} = K_{SV}[Q] + 1 = k_q \tau_0 [Q] \quad (1)$$

where, F_0 is the fluorescence intensity of T80-9-ACANPs in the absence of OHCbl and F is the fluorescence intensity of T80-9-ACANPs when OHCbl is present at a concentration [Q]; K_{sv} is the Stern–Volmer quenching constant and k_q is the quenching rate constant.

The fig. 5 can be seen that the fluorescence intensity of T80-9-ACANPs at 412 nm decreases gradually without any spectral shift with increase in amount of OHCbl from 0.1– 30.0 µM. The obtained experimental data for OHCbl fitted well to the following empirical equation (2).

$$y = 0.4962\,x + 1 \quad (2)$$

From the graph (Fig. 6), the linear relationship in the range of 0.1- 30.0 has a correlation coefficient of $R^2 = 0.9999$ (n=4) and quenching rate constant K_{sv} was found to $4.962 \times 10^5\ M^{-1}$. The limit of detection is calculated by equation (3).

$$LOD = 3.3\sigma / k \quad (3)$$

where, σ is the standard deviation of the y-intercepts of the regression lines and k is the slope of calibration graph. Here, the LOD was 4.65 nM. This suggests that the fluorescence quenching method is more sensitive and selective.

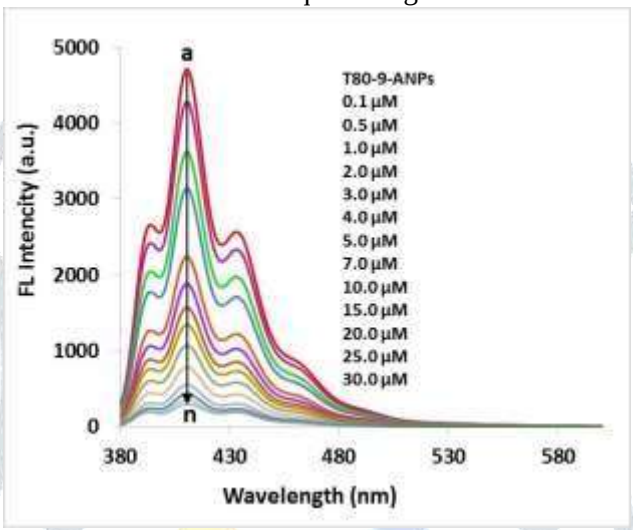

Fig. 5: Fluorescence emission spectra of T80-9-ACANPs in presence of different amounts of OHCbl (0.1-30.0 µM).

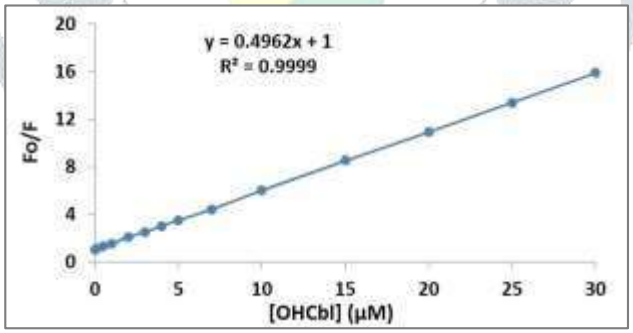

Fig. 6: Stern-Volmer plot of F0/F versus addition of different amounts of OHCbl solution (0.1 – 30.0 µM).

3.2.5 Fluorescence Enhancement Mechanism of T80-9-ACANPs/OHCbl by CN^-

To explore the plausible mechanism of 'turn on' the fluorescence of designed T80-9-ACANPs/OHCbl sensor towards the CN^-, the fluorescence enhancement of T80-9-ACANPs/OHCbl were investigated in the absence (spectrum A) and presence of CN^-. Fig. 7 exhibited the fluorescence spectra of probe with increasing concentration of standard solution of hydrogen cyanide (0.1-30 µM) resulted in the rapid enhancement of fluorescence intensity at λ_{em} = 412 nm (λ_{ex} = 352 nm). The Fig. 8 obtained experimental data for CN^- fitted well to the following empirical equation.

$$F - F_0 = 75.845\,x \quad (4)$$

where F_0 and F are the fluorescence intensities of T80-9-ACANPs/OHCbl in the absence and presence of CN^-. The experimental limit of detection was evaluated as 6.87 nM, which is ~290 times lower than the maximum level (2.0 µM) of cyanide in drinking water permitted by the WHO. According, only CN^- anions induces remarkable fluorescence enhancement due to the probe has ability to bind cyanide ions. Each nanoaggregates based T80-9-ACANPs-OHCbl probe may bind one cyanide ion by replacing the hydroxo ligand linked to the trivalent cobalt ion, to form stable T80-9-

ACANPs-CNCbl. The 'Off-On' fluorescence mechanism of T80-9-ACANPs for recognition of OHCbl and CN^- is schematically represented in scheme 2.

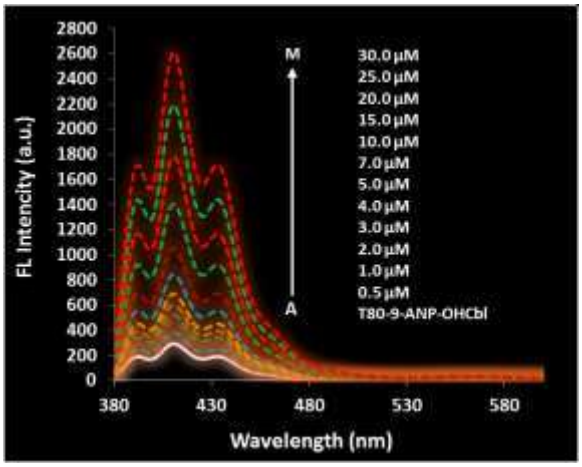

Fig. 7: Fluorescence enhancement spectra of T80-9-ACANPs/OHCbl with increasing concentration of CN^- ion solution (0.5 - 30.0 µM).

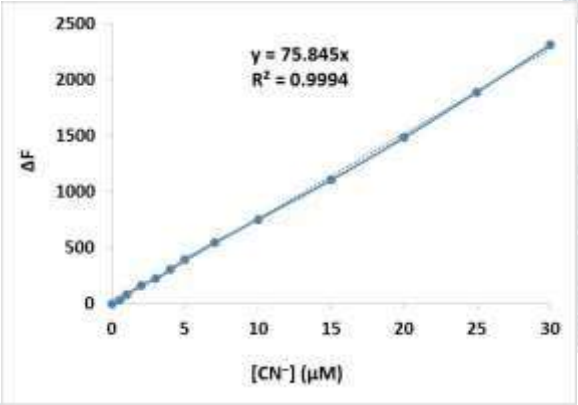

Fig. 8: Calibration curve of ΔF as concentration of CN^- ion.

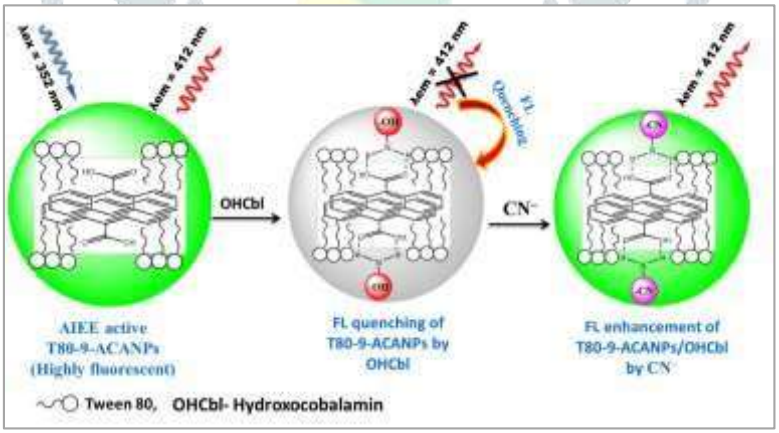

Scheme 2: Proposed scheme of fluorescence "Off-On" recognition system of T80-9-ACANPs for OHCbl and CN^-.

3.2.6 Determination of CN^- in Urine and Environmental Water Samples:

A fluorescent 'Off-On' T80-9-ACANPs/OHCbl based probe was applied for the determination of CN^- from urine samples and environmental water samples. Urine samples from verified healthy anonymous volunteers and patients were obtained from a local hospital and drinking water sample collected from local area (Kolhapur, Maharashtra, India). Impurities and suspended matters from water samples were removed by filtration process using Whatmann filter paper No. 41 and then boiled for 5 minutes to remove dissolved gaseous. Then water samples were spiked with standard solution of HCN at two different concentration levels and were diluted with double distilled water within the working range of 0.5- 30.0 µM of CN^- ions. These samples were analyzed for CN^- content with T80-9-ACANPs/OHCbl fluorescence 'turn on' method. The accuracy and reliability of the method was further ascertained by recovery studies using standard addition method and percent recovery was found in between 98.89 to 99.94 %. The results summarized in Table No. 1,

show good agreement with spiked CN^- ion concentrations and demonstrate that the T80-9-ACANPs/OHCbl is effective sensor for sensing and estimation of CN^- ions from urine and environmental water samples.

Table 1: Determination of CN^- in urine and environmental water samples

Name of the samples studied	Amount of standard CN^- added (µM)	Amount of CN^- found (n=3) (µM)	Recovery of CN^- (n=3) added (%)	RSD (%)	Relative error (%)
Urine sample (*PHC, SUK)	7.0	6.922	98.89	0.0144	-0.07
	15.0	14.877	99.18	0.0066	-0.09
Drinking water sample@	12.0	11.957	99.64	0.0157	-0.36
	20.0	19.987	99.94	0.0112	-0.06

Samples for analysis collected from– *Primary Health Centre (PHC), Shivaji University, Kolhapur, M.S., India, @Rajaram lake, Kolhapur, M.S., India.

4. CONCLUSIONS:

In conclusion, we have successfully prepared and designed fluorescent 'Off-On' T80-9-ACANPs based nano sensor for recognizing hydroxocobalamin and cyanide ion in aqueous media. The blue shifted absorption band of T80-9-ACANPs due to H-aggregated nanostructures shows AIEE at λ_{max} = 412 nm due to hindered molecular rotations favoring radiative decay of nanoaggregates. The linear fitting, R^2 = 0.9999 and 0.9994 of the 'turn-off' and 'turn-on' fluorescence respectively varies at low concentration and provides a considerably high quenching constant 4.962 x 10^5 M^{-1} which is indicative of a very strong interaction of the fluorophore in 'Off-On' fluorescence process. The low limit of detection for quenching and enhancement were calculated to be 4.65 and 6.87 nM respectively. The developed method is simple, rapid, reproducible, selective, affordable and free from the interference of excipients for recognition of hydroxocobalamin and CN^-.

5. REFERENCES:

1. An, B.K.; Kwon, S.K.; Jung, S.D.; Park, S. Y., *J. Am. Chem. Soc.* **2002,** *124* (48), 14410-14415.
2. Dalavi, D. K.; Kamble, A.; Bhopate, D. P.; Mahajan, P. G.; Kolekar, G. B.; Patil, S. R., **2015,** *5* (85), 69371-69377.
3. H.-B. Fu, J.-N. Yao, *J. Am. Chem. Soc.*, 123, **2001**, 1434.
4. Dalavi, D. K.; Bhopate, D.; Bagawan, A.; Gore, A.; Desai, N.; Kamble, A.; Mahajan, P.; Kolekar, G.; Patil, S. R., *Anal. Methods*, **2014,** *6* (17), 6948-6955.
5. H. Yan, H. Li, *Sens. Actuators, B*, 148, **2010**, 81.
6. Dalavi, D. K.; Suryawanshi, S. B.; Kolekar, G. B.; Patil, S. R., *Anal. Methods*, **2018**.
7. D. Horn, J. Rieger, *Angew. Chem. Int. Ed.*, 40, **2001**, 4330.
8. Dalavi, D. K., JOURNAL OF NOVEL RESEARCH AND INNOVATIVE DEVELOPMENT, **2024**, 2(6), a211-a218.
9. Ma, X.; Sun, R.; Cheng, J.; Liu, J.; Gou, F.; Xiang, H.; Zhou, X., *J. Chem. Educ.*, **2016,** *93* (2), 345-350.
10. Gierschner, J.; Lüer, L.; Milián-Medina, B.; Oelkrug, D.; Egelhaaf, H.J., *The Journal of Physical Chemistry Letters*, **2013.**
11. B. Tavares, P. Domingos, P. N. Dias, J. A. Feijó, A. Bicho, *Journal of Experimental Botany*, 62, **2011**, 2273.
12. Shaily, A. Kumar, N. Ahmed, *Ind. Eng. Chem. Res.*, 56, **2017**, 6358.
13. Z. Shojaeifard, B. Hemmateenejad, M. Shamsipur, *ACS Appl. Mater. Interfaces*, 8, (**2016)**, 15177.
14. M. A. Kirk, R. Gerace, K. W. Kulig, *Annals of emergency medicine*, 22, **1993**, 1413.
15. T. Cummings, *Occupational Medicine*, 54, **2004**, 82.
16. E. Jaszczak, Ż. Polkowska, S. Narkowicz, J. Namieśnik, *Environ. Sci. Pollut. Res.*, 24, **2017**, 15929.
17. R. Badugu, J. R. Lakowicz, C. D. Geddes, *J. Am. Chem. Soc.*, 127, **2005**, 3635.
18. L. L. Pearce, E. Lopez Manzano, S. Martinez-Bosch, J. Peterson, *Chem. Res. Toxicol.*, 21, **2008**, 2073.
19. X. Cheng, Y. Zhou, J. Qin, Z. Li, *ACS Appl. Mater. Interfaces*, 4, **2012**, 2133.
20. X. Cheng, R. Tang, H. Jia, J. Feng, J. Qin, Z. Li, *ACS Appl. Mater. Interfaces*, 4, **2012**, 4387.
21. K.-S. Lee, H.-J. Kim, G.-H. Kim, I. Shin, J.-I. Hong, *Org. Lett.*, 10, **2008**, 49.
22. M. Larsen, S. Trapp, *Environ. Sci. Technol.*, 40, **2006**, 1956.
23. Y. G. Timofeyenko, J. J. Rosentreter, S. Mayo, *Analytical Chemistry*, 79, **2007**, 251.
24. M.-J. Peng, Y. Guo, X.-F. Yang, L.-Y. Wang, J. An, *Dyes Pigm.*, 98, **2013**, 327.
25. A. Karmakar, N. Kumar, P. Samanta, A. V. Desai, S. K. Ghosh, *Chemistry-A European Journal*, 22, **2016**, 864.
26. K. H. Jung, K.-H. Lee, *Analytical Chemistry*, 87, **2015**, 9308.
27. N. Phambu, A. S. Meya, E. B. Djantou, E. N. Phambu, P. Kita-Phambu, L. M. Anovitz, *Journal of Agricultural and Food Chemistry*, 55, **2007**, 10135.
28. P. G. Mahajan, N. K. Desai, D. K. Dalavi, D. P. Bhopate, G. B. Kolekar, S. R. Patil, *J. Fluoresc.*, 25, **2015**, 31.
29. S. Li, L. He, F. Xiong, Y. Li, G. Yang, *The Journal of Physical Chemistry B*, 108, **2004**, 10887.
30. B.-K. An, S.-K. Kwon, S.-D. Jung, S. Y. Park, *J. Am. Chem. Soc.*, 124, **2002**, 14410.